Current Biology 17, 1212–1218, July 17, 2007 ©2007 Elsevier Ltd All rights reserved DOI 10.1016/j.cub.2007.06.013

Report

Protein-Tyrosine Phosphatase Sigma Is Associated with Ulcerative Colitis

Aleixo M. Muise,[1,2] Thomas Walters,[1,7] Eytan Wine,[1,2,7] Anne M. Griffiths,[1] Dan Turner,[1] Richard H. Duerr,[4] Miguel D. Regueiro,[4] Bo-Yee Ngan,[3] Wei Xu,[5] Philip M. Sherman,[1,2] Mark S. Silverberg,[6] and Daniela Rotin[2,*]

[1] Division of Gastroenterology, Hepatology, and Nutrition
Department of Pediatrics
[2] Program in Cell Biology and Research Institute
[3] Department of Pathology and the Hospital for Sick Children
University of Toronto
555 University Ave
Toronto, Ontario M5G 1X8
Canada

[4] Division of Gastroenterology, Hepatology, and Nutrition
Department of Medicine
School of Medicine
University of Pittsburgh
UPMC Presbyterian
Mezzanine Level, C-Wing
200 Lothrop Street
Pittsburgh, Pennsylvania 15213

[5] Public Health Sciences and University of Toronto
15-507 Princess Margaret Hospital
610 University Ave
Toronto, Ontario M5G 2M9
Canada

[6] Mount Sinai Hospital Inflammatory Bowel Disease Centre
University of Toronto
600 University Ave
Toronto, Ontario M5G 1X8
Canada

Summary

Inflammatory bowel disease (IBD), a relatively common chronic debilitating intestinal illness, is composed of two broadly defined groups, Crohn's disease (CD) and ulcerative colitis (UC). Although several susceptibility genes for CD have been recently described, susceptibility genes exclusive for UC have not been forthcoming. Here, we show that receptor protein-tyrosine phosphatase sigma (PTPRS—encoding PTPσ) knockout mice spontaneously develop mild colitis that becomes severe when challenged with two known inducers of colitis. We also demonstrate that E-cadherin and β-catenin, two important adherens junction proteins involved in maintenance of barrier defense in the colon, act as colonic substrates for PTPσ. Furthermore, we show that three SNPs (rs886936, rs17130, and rs8100586) that flank exon 8 in the human PTPRS gene are associated with UC. The presence of these SNPs is associated with novel splicing that removes the third immunoglobulin-like domain (exon 9) from the extracellular portion of PTPσ, possibly altering dimerization or ligand recognition. We propose that polymorphisms in the human PTPRS gene lead to ulcerative colitis.

Results and Discussion

The PTPRS-knockout (KO) mice we previously generated display features consistent with human IBD. Mice that survive the high neonatal mortality suffer severe cachexia [1, 2]. Surviving mice appear phenotypically normal except for mild colitis and significant growth failure compared to their wild-type (WT) littermates [1, 3]. In this mouse model, we used the LacZ insert knocked in to show that PTPRS was expressed in the colon (Figures S1A–S1C in the Supplemental Data available online).

We confirmed that the PTPRS-KO mice spontaneously develop colitis (histological score [4] of 1.5; Figure 1A_b and Figure S1F) and further described crypt branching and architectural distortion that was evident on transmission electron micrographs (Figure S1H).

To determine whether the PTPRS-KO mice were further susceptible to experimental colitis, we treated PTPRS-KO mice and wild-type littermates with dextran sodium sulfate (DSS), an established colitis model [5]. As shown in Figure 1D, the PTPRS-KO mice exhibited rectal bleeding within 3 days of DSS treatment, and 100% of the KO mice were bleeding by day 6 compared with 18% of the wild-type group ($p < 0.001$, log rank test). In addition, the PTPRS-KO mice lost significantly more weight (Figure 1B_a) than their littermates ($p = 0.01$, Wilcoxon rank sum test). These results, summarized in a disease activity index (DAI) score [4], show that the PTPRS-KO mice developed severe colitis in this experimental model (Figure 1C_a). This effect was most dramatically seen in the distal colon as severe ulcers and necrosis (Figure 1A_a) that were significantly worse in the PTPRS-KO colon, compared with the wild-type controls (histological score; $p = 0.001$, Wilcoxon rank sum test; Figure 1A_b). The PTPRS-KO mice also had significantly more bacteria translocated to mesenteric lymph nodes compared to the wild-type ($p = 0.009$, Fisher's exact test; Figure 1E), again emphasizing the worsening of the existing colitis in these mice.

To further demonstrate that PTPRS-KO mice have an increased susceptibility to colitis, we used the *Citrobacter rodentium* experimental model of colitis [6]. As shown in Figure 1B_b, the PTPRS-KO mice showed significant weight loss, whereas the wild-type mice (and untreated PTPRS-KO mice, not shown) continued to gain weight during the entire experimental period ($p < 0.001$, Wilcoxon rank sum test). The PTPRS mice had significantly worse median DAI ($p < 0.001$, Wilcoxon rank sum test; Figure 1C_b) and histological scores ($p < 0.001$,

*Correspondence: drotin@sickkids.ca
[7] These authors contributed equally to this work.

Wilcoxon rank sum test; Figure 1A$_b$) compared to wild-type littermates.

Transmission electron micrographs showed that the PTPRS-KO mice challenged with *C. rodentium* had increased luminal bacterial colonization (Figure 2A), especially within the colonic crypts; such an increased colonization is rarely observed in healthy colons [7]. This finding was supported by the decrease in bacterial clearance found in the PTPRS-KO mice compared to the wild-type ($p < 0.04$, Fisher's exact test; data not shown). Furthermore, the presence of luminal bacteria was associated with damage to the epithelial surface, resulting in increased shedding (anoikis) of epithelial cells into the gut lumen (Figure 2B). Anoikis is known to be increased in IBD and is associated with early loss of E-cadherin in enterocytes [8, 9].

We recently identified N-cadherin and β-catenin as in vivo substrates for PTPσ in the nervous system [10]. To further understand the pathophysiology by which PTPσ caused colitis in these KO mice, we performed substrate-trapping experiments [11] to test whether E-cadherin and β-catenin were in vivo substrates for PTPσ in the colon. Figure 2C shows that these proteins might be colonic substrates for PTPσ. In support, we found that E-cadherin is hypertyrosine phosphorylated in the colons of the PTPRS-KO mice relative to sibling controls (Figure 2D). Both E-cadherin [12, 13] and β-catenin [13] are involved in colonic physiology, with a cadherin-dominant-negative-mouse model expressed in the gut causing intestinal inflammation [14]. Phosphorylation of E-cadherin [15, 16] and β-catenin [17–19] results in cellular redistribution of E-cadherin and cell disassociation leading to disassembly of the adherens junction [20]. Taken together, these findings point to a potential role for PTPσ in maintaining the adherens-junction proteins E-cadherin/β-catenin in a dephosphorylated state and, thereby, enhancing barrier-defense integrity in the colon. Alternatively, loss of PTPσ may lead to the disruption of migration along the crypt-villus axis and increased apoptosis, similar to loss E-cadherin in the cadherin-KO-mouse model [21, 22]. Because PTPRS is significantly expressed in the muscularis of the large bowel, it is possible that PTPσ may also be involved in dysmotility seen in IBD patients [23].

Because the PTPRS gene is located on chromosome 17 in the mouse genome and in a region known to be associated with colitis in mice [24], we investigated, by using a candidate-gene approach, whether PTPRS also played a role in human IBD. Interestingly, PTPRS is located in a syntenic block that is on human chromosome 19p13.3 [25] and that is also associated with human colitis (IBD6 locus). IBD6 was identified in a genome-wide scan of Canadian families and demonstrated linkage to IBD, UC, and CD [26]. The importance of IBD6 as a susceptibility locus has been subsequently confirmed by genome scan meta-analysis [27]. To date, no susceptibility genes for IBD in this locus have been defined [28, 29]. Although MYO9B (located on chromosome 19) showed association with CD and UC, it does not contribute to the original IBD6 observation of linkage because of the low contribution of sibling risk [30]. PTPRS is located in the region of maximum linkage in IBD6 (D19S591/D5S247-GATA21G05) [26]. To determine whether PTPRS is a susceptibility gene for IBD, we first identified 42 SNPs (34 SNPs identified from the HapMap accounting for all Tag SNPs and non-Tag SNPs, and eight additional nonsynonomous SNPs) covering the entire PTPRS gene and flanking regions (chromosome 19, 5140–5259 kb). IBD trios (patients and parents; 409 nuclear families containing 1276 persons; summarized in Table S1) from the Hospital for Sick Children and Mount Sinai Hospital in Toronto, Canada, were the genotyped for 33 of these SNPs (nine SNPs, including all eight additional nonsynonymous SNPs and one SNP flanking PTPRS, had minor allele frequency of <1%).

Initial studies of the 33 SNPs with transmission disequilibrium testing (FBAT-e) showed an association with IBD and UC (Tables S5 and S6), with no association with CD (Table S7). Figure 3 shows the linkage-disequilibrium pattern for all 33 SNPs for UC. We then genotyped three SNPs (rs886936, rs17130, and rs8100586) in an additional 37 UC trios from Pittsburgh and performed a joint analysis by using 164 nuclear families containing 175 UC-affected offspring (Toronto and Pittsburgh Trios). Three SNPs, rs886936, rs17130, and rs8100586, showed significant association with UC (additive modeling FBAT-e: $p = 0.0039$, 0.030, and 0.0071, respectively; recessive modeling FBAT-e: $p = 0.0062$, 0.050, and 0.00051 respectively). The three-marker haplotype (rs886936, rs17130, and rs8100586) for the combined trios was also significant for association with UC (HBAT-e; $p = 0.009$). Although the three SNPs are in strong linkage disequilibrium with one another, only rs17130 and rs8100586 form a block (block 5; Figure 3). To determine whether either of these two SNPs can explain the association observed in block 5, we applied conditional haplotype-based likelihood testing [31]. This conditional analysis showed that rs8100586 can explain the total association of these two SNPs, whereas rs17130 cannot. In addition, we added rs886936 as an explanatory variable to the single SNP regression model of rs8100586 to determine whether these two SNP have an independent effect. Both rs886936 and rs8100586 showed significant associations in the analysis. The additional analyses suggested that rs886936 and rs8100586 affect disease risk independently, whereas rs17130 has no effect. Permutation testing to account for multiple testing yielded significant values for the two-independent SNP haplotype and rs886936 and rs8100586 singly ($p = 0.018$, 0.020, and 0.038, respectively; 100,000 permutations with Haploview). There was no further association with the risk genotypes and a number of covariants (family history, Judaism, gender, or disease location; all $p > 0.05$, Table S2). Similarly, no association was seen within the subgroup of Crohn's colitis patients. Further larger replication studies may provide a specific UC phenotype not described here and determine whether PTPRS is associated with Crohn's colitis. Taken together, the animal model and genetic studies indicate that PTPRS may be a susceptibility gene for UC in the IBD6 locus.

These SNPs are located in a physiologically important region of PTPRS, a region that is highly regulated by alternate splicing of exon 8 (termed a microexonB [meB])—a spacer sequence encoding the sequence ELRE (Figure 4B and Figure S2). To determine whether

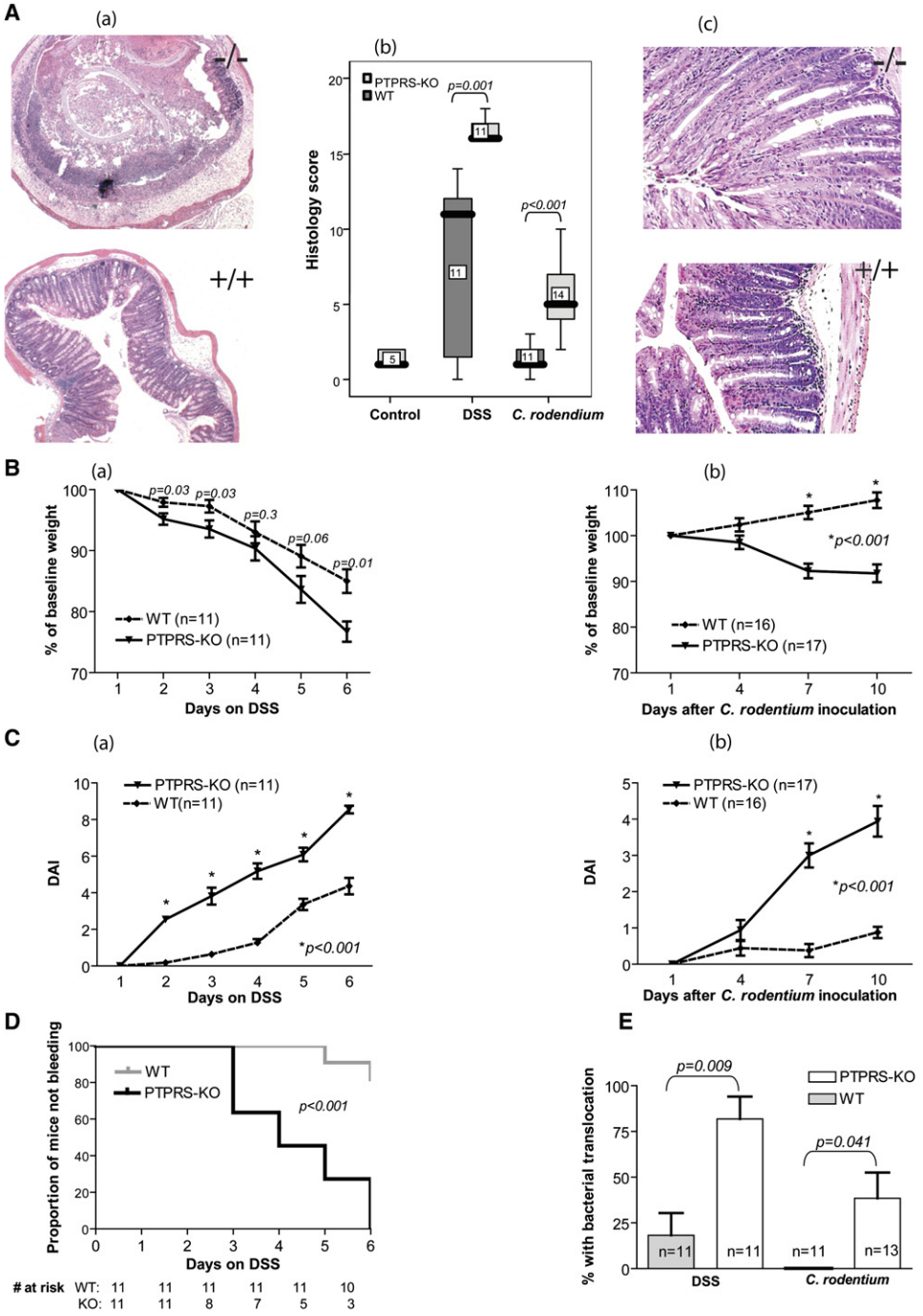

Figure 1. Increased Susceptibility to Colitis in PTPσ Knockout Mice in Two Experimental Models

(A) Histology results. (A_a) shows the histology of DSS-treated mice H and E staining of the distal colon after 6 days of 3% DSS treatment of wild-type mice (magnification 10×; bottom panel: labeled, +/+) compared with PTPRS-KO (magnification 10×; top panel: labeled, −/−) littermates. Wild-type mice show crypt thickening associated with DSS-induced colitis. PTPRS-KO mice show severe colitis with profound ulceration and necrosis of bowel. (A_b) shows the histology score of DSS-treated mice and *C. rodentium* inoculated mice. All scores are compared to normal values determined by scoring of ten wild-type mice. The left column shows untreated PTPRS-KO mice. Center columns show a significant difference in the median histological score of the PTPRS-KO mice compared wild-type mice treated with 3% DSS (16 [IQR 16–17] and 11 [IQR 1.5–12], respectively; p = 0.001, Wilcoxon rank sum test). A similar difference was found between the histological scores after *C. rodentium* inoculation of PTPRS-KO and wild-type mice (5 [IQR 4–7] versus 1 [IQR 1–2]; p < 0.001, Wilcoxon rank sum test). (A_c) shows the histology of *C. rodentium* inoculated mice. H and E staining of the distal colon 10 days after *C. rodentium* inoculation of wild-type mice (magnification 25×; bottom panel: labeled, +/+) compared with PTPRS-KO (magnification 25×; top panel: labeled, −/−) littermates is shown. Wild-type mice show crypt hyperplasia associated with colitis. PTPRS-KO mice show substantially increased crypt hyperplasia.

(B) Weight loss of DSS-treated mice and *C. rodentium* inoculated mice. (C_a) shows that PTPRS-KO mice treated with 3% DSS lost significantly more weight than the wild-type mice after six days of DSS treatment (p values as shown in the figure, Wilcoxon rank sum). In order to compare the overall weights of the wild-type and the PTPRS-KO mice, we calculated the area under the curves (AUC) for each observation throughout the time period. The PTPRS-KO mice had significantly smaller AUC (448 [435–437]) than the wild-type mice (478 [453–481]), implying that overall, the

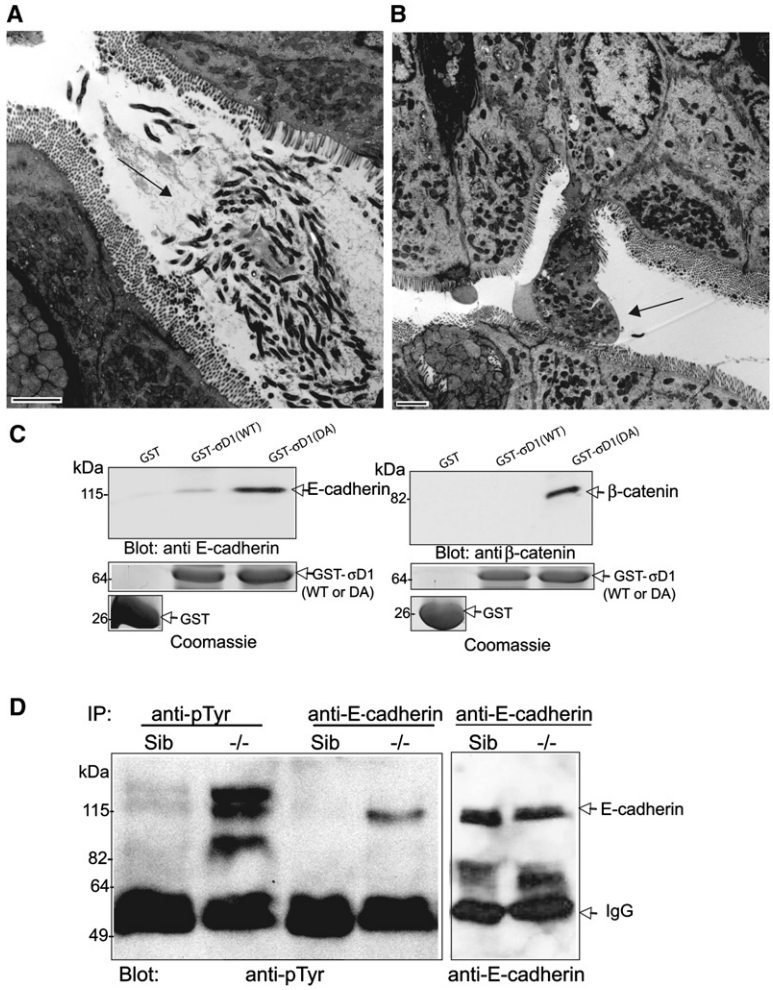

Figure 2. Abnormalities in the Large Bowel after *C. rodentium* Inoculation, and PTPσ Substrate Identification

(A and B) TEM of distal colon of PTPRS-KO mice after *C. rodentium* inoculation. Transmission electron micrograph of the distal colon of PTPRS-KO mice, 10 days after *C rodentium* infection, is shown. (A) shows *C rodentium* in the lumen of the colon (arrow). (B) shows increased anoikis (arrow). Scale bars represent 2 μm.

(C) Substrate-trapping assay identifying E-cadherin and β-catenin as colonic substrates for PTPσ. Catalytically-inactive trapping mutant of PTPσ [GST-σD1(DA)], or wild-type controls [GST-σD1(WT)], were incubated with lysates from colons of the PTPRS-KO mice, and the precipitates were immunoblotted for E-cadherin (left panel) and β-catenin (right panel). The controls fusion proteins used for the pulldown assays [GST-σD1(DA), GST-σD1(WT), or GST alone] are shown below each panel.

(D) E-cadherin is hyper-Tyr-phosphorylated in colons of the PTPσ-KO mice. Colon from PTPRS-KO mice (−/−) or wild-type sibling (Sib) controls were lysed, and proteins in the lysate were immunoprecipitated (IP) with either pTyr or E-cadherin antibodies. The IPs were then immunoblotted with either phosphotyrosine (anti-pTyr) or E-cadherin antibodies.

the region containing the SNPs found here to be associated with UC leads to alternative splicing, we compared genotyped immortalized lymphoblast-cell lines derived from individuals from the Centre d'Etude du Polymorphisme Humain. Thus, we compared three individuals with the three-marker haplotype associated with UC with three individuals homozygous for the nucleotide not associated with UC. mRNA was isolated from the lymphoblast-cell lines, and a DNA fragment corresponding to amino acids 191–371 of PTPσ was amplified with PCR. All three control individuals had the expected 168 amino acid sequence that was a 100% match with either isoform-2 or -3 (Figure 4A and Figure S2C). In contrast, the individuals with the three-marker haplotype associated with UC had a novel splice variant of isoform-1 that removed meB and exon 9, along with the normal isoforms-2 and -3 (Figure 4A and Figure S2C). This novel splicing resulted in the deletion of the entire third immunoglobulin domain in the ectodomain of the PTPσ protein (Figure 4B). This splice variant of exon 9 is only in-frame in isoform-1, which is the predominant form of PTPRS in the colon [32]. Because this splicing does not occur in the shorter forms of PTPRS (isoform-3 and -4) found in the brain [32], the neurological abnormalities associated with PTPRS-KO mice [1, 2] are not expected or seen in patients with UC. Although the

PTPRS-KO mice lost significantly more weight than the KO mice (Wilcoxon rank sum test; $p = 0.013$). (C_b) shows that PTPRS-KO mice inoculated with *C. rodentium* had significant weight loss, whereas the wild-type mice continued to gain weight during the experiment period ($p < 0.001$ at day 7 and 10, Wilcoxon rank sum test; error bars represent SEM).

(C) Disease activity index (DAI) of DSS-treated mice and *C. rodentium* inoculated mice. (B_a) shows that the DAI score was significantly higher in the PTPRS-KO mice compared with the wild-type mice from the second day to the end of DSS treatment (all $p < 0.001$, Wilcoxon rank sum test). Control untreated PTPRS-KO and wild-type mice had a DAI score of 0. (B_b) shows that the PTPRS-KO mice had a significantly worse median DAI score on days 7 and 10 after *C. rodentium* inoculation (both $p < 0.001$, Wilcoxon rank sum test; error bars represent SEM).

(D) Bleeding in DSS-treated mice. Four of 11 PTPRS-KO mice (36%) began to bleed within 3 days of DSS treatment compared to none of the wild-type mice (0/11). After 6 days, all (100%) PTPRS-KO mice compared to only two of the wild-type mice (18%) were bleeding ($p < 0.001$, log rank test = 16.9, hazard ratio = 0.1 (95% [CI 0.02–0.25]; error bars represent SEM).

(E) Bacterial translocation in DSS-treated mice and *C. rodentium* inoculated mice. PTPRS mice treated with 3% DSS (left panel) had significantly more bacteria translocated to mesenteric lymph nodes compared with the wild-type (9/11 [82%] versus 2/11 [18%]; $p = 0.009$, Fisher's exact test). PTPRS-KO mice inoculated with *C. rodentium* (right panel) had significantly more bacteria translocated to mesenteric lymph nodes compared with the wild-type (5/13 [39%] versus 0/11 [0%]; $p = 0.041$, Fisher's exact test; error bars represent SEM).

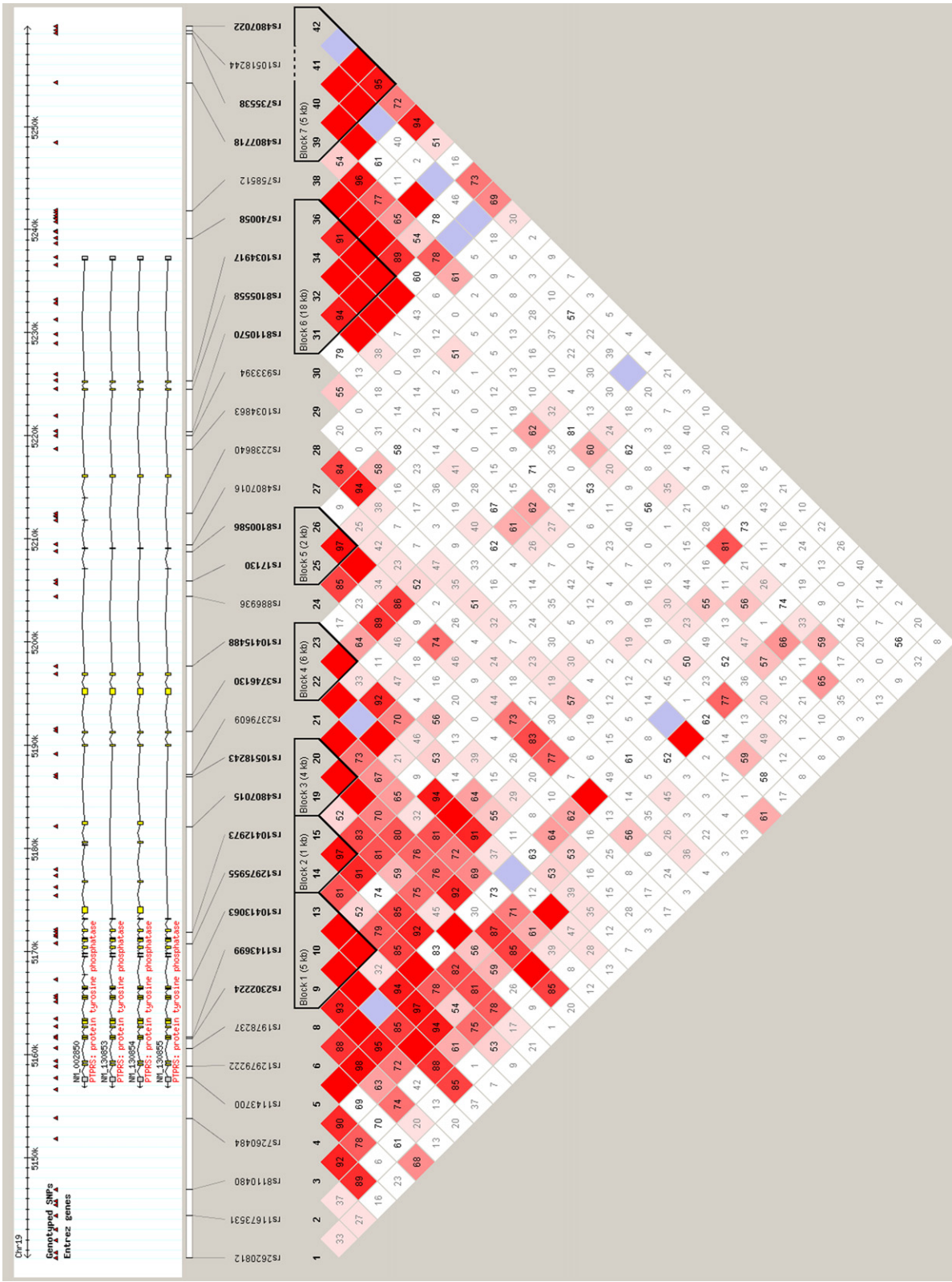

Figure 3. LD Plot of SNPs Covering the Entire PTPRS Gene

Linkage-disequilibrium pattern across the PTPRS gene and flanking regions for the 33 SNPs. The values are 100 × D′ with the blank squares representing D′ of 1.0. Seven haplotypes are shown as predicted by haploview.

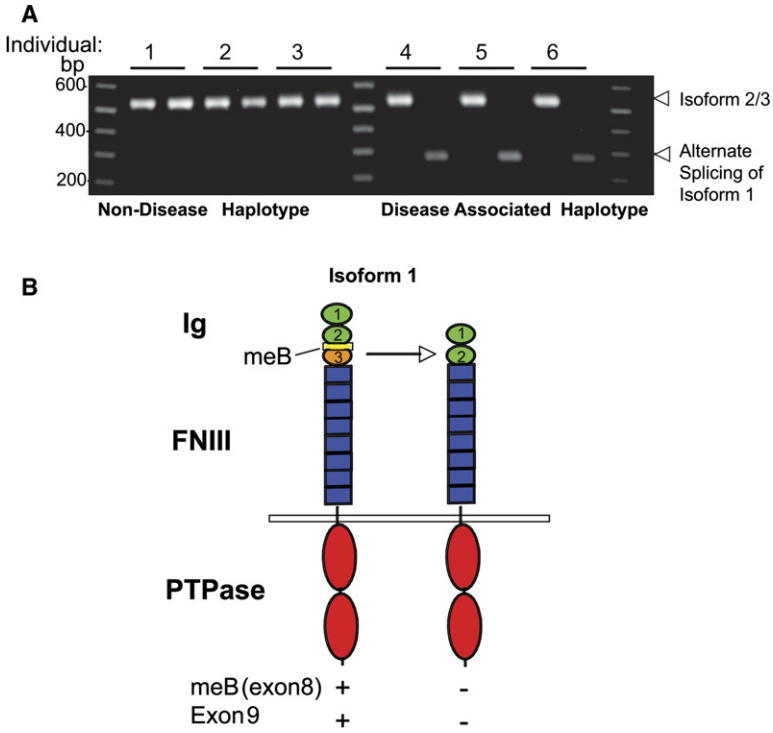

Figure 4. Alternate Splicing of PTPRS

(A) PCR analysis showing alternate splicing of meB and exon 9. Three healthy control individuals from the "Centre d'Etude du Polymorphisme Humain" (CEPH 1334.13, 1340.11, and 1340.12) with homozygote C nucleotide at rs8100856 and either GG or AG at rs17130 and rs886936 were compared with three individuals (CEPH 1340.01, 1344.13, and 1362.02) with homozygote nucleotide A for all SNPs resulting in the three-marker haplotype found to be associated with UC. PCR product isolated from the control individuals (left) and the three-marker haplotype associated with UC (right) are shown. The large fragment corresponds to isoform 2 and 3, and the smaller fragment corresponds to the alternate splicing of exon 8 and 9 in isoform 1.

(B) Novel alternate splicing of meB and exon 9. Alternate splicing in rs17130, rs886939, and rs8100586 three-marker haplotype is shown. Exon 9, Ig-like domain 3 (Ig3, shown in orange), is spliced out along with meB (yellow, usually found in this isoform-1). This splicing variant is only inframe in isoform-1.

function of the Ig-like domain of PTPσ is unknown, we speculate that it plays a role in either dimerization or ligand binding of PTPσ [33], similar to the alternate splicing in PTPRC (CD45) that is associated with multiple sclerosis [34, 35]. These results indicate that these polymorphisms may disrupt the balance of splice variants in the colon and that alternate splicing of exon 9 may help explain the association with colitis described here.

In summary, we show here that SNPs flanking exon 8 within the PTPRS gene have significant association with UC. The three-marker haplotype associated with UC results in novel alternate splicing of meB and exon 9. This novel splicing completely removes the third immunoglobulin like (Ig-like) domain of PTPσ, possibly altering ligand recognition or dimerization that may be important for ligand binding. PTPRS is known to be expressed in the human colon [32], and we demonstrate that PTPRS-KO mice develop spontaneous mild colitis and are susceptible to induced colitis. Taken together, our work identifies PTPRS as a novel gene associated with ulcerative colitis and provides important insight into the pathogenesis of this disease.

Supplemental Data

Experimental Procedures, two figures, and seven tables are available at http://www.current-biology.com/cgi/content/full/17/14/1212/DC1/.

Acknowledgments

Thanks to Joanne Stempak, Chen Lu, and Angela Griffin for technical support. This work was supported by the Canadian Institute of Health Research (CIHR) to D.R., the Crohn's Colitis Foundation of Canada (CCFC) to A.M.G. and D.R., and a Thrasher Research Fund New Investigators Grant to A.M.M. A.M.M. is supported by a fellowship from the Canadian Child Health Clinician Scientist Program (Strategic Training Initiatives in Health Research Program—CIHR). T.W., E.W., and D.T. are supported by fellowships from the Canadian Gastroenterology Association/CIHR (E.W., Astra-Zeneca Partnered; T.W. and D.T., CCFC Partnered). A.M.M., E.W., and D.T. are supported by Post-Graduate Medical Education Awards, Faculty of Medicine, University of Toronto. D.R. and P.M.S. hold a Canada Research Chair (Tier I) from the CFI/CIHR.

Received: April 13, 2007
Revised: June 4, 2007
Accepted: June 5, 2007
Published online: July 5, 2007

References

1. Wallace, M.J., Batt, J., Fladd, C.A., Henderson, J.T., Skarnes, W., and Rotin, D. (1999). Neuronal defects and posterior pituitary hypoplasia in mice lacking the receptor tyrosine phosphatase PTPsigma. Nat. Genet. *21*, 334–338.
2. Elchebly, M., Wagner, J., Kennedy, T.E., Lanctot, C., Michaliszyn, E., Itie, A., Drouin, J., and Tremblay, M.L. (1999). Neuroendocrine dysplasia in mice lacking protein tyrosine phosphatase sigma. Nat. Genet. *21*, 330–333.
3. Batt, J., Asa, S., Fladd, C., and Rotin, D. (2002). Pituitary, pancreatic and gut neuroendocrine defects in protein tyrosine phosphatase-sigma-deficient mice. Mol. Endocrinol. *16*, 155–169.
4. Van der Sluis, M., De Koning, B.A., De Bruijn, A.C., Velcich, A., Meijerink, J.P., Van Goudoever, J.B., Buller, H.A., Dekker, J., Van Seuningen, I., Renes, I.B., and Einerhand, A.W. (2006). Muc2-deficient mice spontaneously develop colitis, indicating that MUC2 is critical for colonic protection. Gastroenterology *131*, 117–129.
5. Egger, B., Bajaj-Elliott, M., MacDonald, T.T., Inglin, R., Eysselein, V.E., and Buchler, M.W. (2000). Characterisation of acute murine dextran sodium sulphate colitis: Cytokine profile and dose dependency. Digestion *62*, 240–248.
6. Hansen, K.K., Sherman, P.M., Cellars, L., Andrade-Gordon, P., Pan, Z., Baruch, A., Wallace, J.L., Hollenberg, M.D., and Vergnolle, N. (2005). A major role for proteolytic activity and proteinase-activated receptor-2 in the pathogenesis of infectious colitis. Proc. Natl. Acad. Sci. USA *102*, 8363–8368.
7. van der Waaij, L.A., Harmsen, H.J., Madjipour, M., Kroese, F.G., Zwiers, M., van Dullemen, H.M., de Boer, N.K., Welling, G.W.,

and Jansen, P.L. (2005). Bacterial population analysis of human colon and terminal ileum biopsies with 16S rRNA-based fluorescent probes: Commensal bacteria live in suspension and have no direct contact with epithelial cells. Inflamm. Bowel Dis. *11*, 865–871.

8. Fouquet, S., Lugo-Martinez, V.H., Faussat, A.M., Renaud, F., Cardot, P., Chambaz, J., Pincon-Raymond, M., and Thenet, S. (2004). Early loss of E-cadherin from cell-cell contacts is involved in the onset of Anoikis in enterocytes. J. Biol. Chem. *279*, 43061–43069.
9. Joseph, R.R., Yazer, E., Hanakawa, Y., and Stadnyk, A.W. (2005). Prostaglandins and activation of AC/cAMP prevents anoikis in IEC-18. Apoptosis *10*, 1221–1233.
10. Siu, R., Fladd, C., and Rotin, D. (2007). N-Cadherin is an in vivo substrate for protein tyrosine phosphatase sigma (PTP{sigma}) and participates in PTP{sigma}-mediated inhibition of axon growth. Mol. Cell. Biol. *27*, 208–219.
11. Flint, A.J., Tiganis, T., Barford, D., and Tonks, N.K. (1997). Development of "substrate-trapping" mutants to identify physiological substrates of protein tyrosine phosphatases. Proc. Natl. Acad. Sci. USA *94*, 1680–1685.
12. Jankowski, J.A., Bedford, F.K., Boulton, R.A., Cruickshank, N., Hall, C., Elder, J., Allan, R., Forbes, A., Kim, Y.S., Wright, N.A., and Sanders, D.S. (1998). Alterations in classical cadherins associated with progression in ulcerative and Crohn's colitis. Lab. Invest. *78*, 1155–1167.
13. Karayiannakis, A.J., Syrigos, K.N., Efstathiou, J., Valizadeh, A., Noda, M., Playford, R.J., Kmiot, W., and Pignatelli, M. (1998). Expression of catenins and E-cadherin during epithelial restitution in inflammatory bowel disease. J. Pathol. *185*, 413–418.
14. Hermiston, M.L., and Gordon, J.I. (1995). Inflammatory bowel disease and adenomas in mice expressing a dominant negative N-cadherin. Science *270*, 1203–1207.
15. Luber, B., Candidus, S., Handschuh, G., Mentele, E., Hutzler, P., Feller, S., Voss, J., Hofler, H., and Becker, K.F. (2000). Tumor-derived mutated E-cadherin influences beta-catenin localization and increases susceptibility to actin cytoskeletal changes induced by pervanadate. Cell Adhes. Commun. *7*, 391–408.
16. Roura, S., Miravet, S., Piedra, J., Garcia de Herreros, A., and Dunach, M. (1999). Regulation of E-cadherin/Catenin association by tyrosine phosphorylation. J. Biol. Chem. *274*, 36734–36740.
17. Hu, P., O'Keefe, E.J., and Rubenstein, D.S. (2001). Tyrosine phosphorylation of human keratinocyte beta-catenin and plakoglobin reversibly regulates their binding to E-cadherin and alpha-catenin. J. Invest. Dermatol. *117*, 1059–1067.
18. Kinch, M.S., Clark, G.J., Der, C.J., and Burridge, K. (1995). Tyrosine phosphorylation regulates the adhesions of ras-transformed breast epithelia. J. Cell Biol. *130*, 461–471.
19. Liu, D., el-Hariry, I., Karayiannakis, A.J., Wilding, J., Chinery, R., Kmiot, W., McCrea, P.D., Gullick, W.J., and Pignatelli, M. (1997). Phosphorylation of beta-catenin and epidermal growth factor receptor by intestinal trefoil factor. Lab. Invest. *77*, 557–563.
20. Staddon, J.M., Herrenknecht, K., Smales, C., and Rubin, L.L. (1995). Evidence that tyrosine phosphorylation may increase tight junction permeability. J. Cell Sci. *108*, 609–619.
21. Hermiston, M.L., and Gordon, J.I. (1995). In vivo analysis of cadherin function in the mouse intestinal epithelium: Essential roles in adhesion, maintenance of differentiation, and regulation of programmed cell death. J. Cell Biol. *129*, 489–506.
22. Hermiston, M.L., Wong, M.H., and Gordon, J.I. (1996). Forced expression of E-cadherin in the mouse intestinal epithelium slows cell migration and provides evidence for nonautonomous regulation of cell fate in a self-renewing system. Genes Dev. *10*, 985–996.
23. Vrees, M.D., Pricolo, V.E., Potenti, F.M., and Cao, W. (2002). Abnormal motility in patients with ulcerative colitis: The role of inflammatory cytokines. Arch. Surg. *137*, 439–445.
24. Kozaiwa, K., Sugawara, K., Smith, M.F., Jr., Carl, V., Yamschikov, V., Belyea, B., McEwen, S.B., Moskaluk, C.A., Pizarro, T.T., Cominelli, F., and McDuffie, M. (2003). Identification of a quantitative trait locus for ileitis in a spontaneous mouse model of Crohn's disease: SAMP1/YitFc. Gastroenterology *125*, 477–490.
25. Wagner, J., Gordon, L.A., Heng, H.H., Tremblay, M.L., and Olsen, A.S. (1996). Physical mapping of receptor type protein tyrosine phosphatase sigma (PTPRS) to human chromosome 19p13.3. Genomics *38*, 76–78.
26. Rioux, J.D., Silverberg, M.S., Daly, M.J., Steinhart, A.H., McLeod, R.S., Griffiths, A.M., Green, T., Brettin, T.S., Stone, V., Bull, S.B., et al. (2000). Genomewide search in Canadian families with inflammatory bowel disease reveals two novel susceptibility loci. Am. J. Hum. Genet. *66*, 1863–1870.
27. van Heel, D.A., Fisher, S.A., Kirby, A., Daly, M.J., Rioux, J.D., and Lewis, C.M. (2004). Inflammatory bowel disease susceptibility loci defined by genome scan meta-analysis of 1952 affected relative pairs. Hum. Mol. Genet. *13*, 763–770.
28. van Heel, D.A., Dechairo, B.M., Dawson, G., McGovern, D.P., Negoro, K., Carey, A.H., Cardon, L.R., Mackay, I., Jewell, D.P., and Lench, N.J. (2003). The IBD6 Crohn's disease locus demonstrates complex interactions with CARD15 and IBD5 disease-associated variants. Hum. Mol. Genet. *12*, 2569–2575.
29. Tello-Ruiz, M.K., Curley, C., DelMonte, T., Giallourakis, C., Kirby, A., Miller, K., Wild, G., Cohen, A., Langelier, D., Latiano, A., et al. (2006). Haplotype-based association analysis of 56 functional candidate genes in the IBD6 locus on chromosome 19. Eur. J. Hum. Genet. *14*, 780–790.
30. van Bodegraven, A.A., Curley, C.R., Hunt, K.A., Monsuur, A.J., Linskens, R.K., Onnie, C.M., Crusius, J.B., Annese, V., Latiano, A., Silverberg, M.S., et al. (2006). Genetic variation in myosin IXB is associated with ulcerative colitis. Gastroenterology *131*, 1768–1774.
31. Purcell, S., Daly, M.J., and Sham, P.C. (2007). WHAP: Haplotype-based association analysis. Bioinformatics *23*, 255–256.
32. Endo, N., Rutledge, S.J., Opas, E.E., Vogel, R., Rodan, G.A., and Schmidt, A. (1996). Human protein tyrosine phosphatase-sigma: Alternative splicing and inhibition by bisphosphonates. J. Bone Miner. Res. *11*, 535–543.
33. Lajus, S., and Lang, J. (2006). Splice variant 3, but not 2 of receptor protein-tyrosine phosphatase sigma can mediate stimulation of insulin-secretion by alpha-latrotoxin. J. Cell. Biochem. *98*, 1552–1559.
34. Lynch, K.W., and Weiss, A. (2001). A CD45 polymorphism associated with multiple sclerosis disrupts an exonic splicing silencer. J. Biol. Chem. *276*, 24341–24347.
35. Jacobsen, M., Schweer, D., Ziegler, A., Gaber, R., Schock, S., Schwinzer, R., Wonigeit, K., Lindert, R.B., Kantarci, O., Schaefer-Klein, J., et al. (2000). A point mutation in PTPRC is associated with the development of multiple sclerosis. Nat. Genet. *26*, 495–499.